Journal of Achievements in Materials and Manufacturing Engineering
VOLUME 37
ISSUE 2
December
2009

Exploring laser-guided metal deposition through a microbe metabolite

H. Hocheng*, K.E. Chang, J.H. Chang, J.C. Wang
[a] Department of power mechanical engineering,
National Tsing Hua University, Taiwan R.O.C
* Corresponding author: E-mail address: hocheng@pme.nthu.edu.tw

Received 20.09.2009; published in revised form 01.12.2009

Manufacturing and processing

ABSTRACT

Purpose: The purpose of the paper is to describe exploring laser-guided metal deposition through a microbe metabolite.
Design/methodology/approach: A maskless micro-fabrication of laser-guided deposition process through the metabolite of Acidophilic bacteria Thiobacillus ferrooxidans (T.f.) is explored.
Findings: The authors have conducted an analysis of the metal deposition process using the point thermal-source of the Nd:YAG laser through the metabolite of Acidophilic bacteria Thiobacillus. An analytical model adopting the moving point heat source on the substrate and heat transfer conditions is presented. The thermal field generated by the laser input energy is investigated.
Practical implications: Though the mechanism of the laser-assisted deposition process is not fully revealed by biologist yet, the current model provides a means of control of the line deposition of metals.
Originality/value: Based on the fundamental knowledge of how the line width varies with laser power and scanning speed, more investigation of the mini-scale heat convection and the threshold temperature of chemical reaction is expected in the future for further understanding of this novel metal deposition method triggered and written by laser.
Keywords: Laser; Metal Deposition; Micro-fabrication; Microbe; Metabolit

Reference to this paper should be given in the following way:
H. Hocheng, K.E. Chang, J.H. Chang, J.C. Wang, Exploring laser-guided metal deposition through a microbe metabolite, Journal of Achievements in Materials and Manufacturing Engineering 37/2 (2009) 639-643.

1. Introduction

Solid freeform fabrication (SFF) is a technique for producing solid parts by transferring energy and/or material to specific locations on a substrate layer by layer. The techniques such as laser engineered net shaping (LENS®) [1], selective laser sintering [2] (SLS, a registered trademark of 3D Systems, Inc.), stereolithography [3] and laser assisted chemical vapor deposition (LCVD) [4] are the examples of layered and additive fabrication processes using laser as the source of energy.

Surface processing with lasers which enable the localized metal deposition of copper material through Thiobacillus ferrooxidans metabolite offers an advantage of minimal environmental impact compared to other laser-assisted chemical vapor deposition. Thiobacillus ferrooxidans is an autotrophic acidophilic bacterium and its growth can be supported by the oxidation of inorganic ferrous to ferric iron [5,6]. The mechanism of displacement deposition is analogous to the autocatalytic electroless deposition (AED), but the reaction does not require any further chemical reducing agent besides ferric iron. This technique can be used to deposit a copper line on the same substrate with the resolution of a micrometer. It has the concerns of controlling the beam parameters, adhesion of copper and vapour confusion during the deposition process. Basically, the

substrate must be copper acting as copper ionic source oxidized by ferric iron of T.f. metabolite with a more positive standard electrode potential and the copper reduction triggered by laser excitation. The authors have conducted an analysis of the metal deposition process on copper surface using the point thermal-source of the Nd:YAG laser through the metabolite of Acidophilic bacteria Thiobacillus.

2. Thermal analysis of deposition

The laser beam size cast on substrate is defined by the diameter of 50% of energy intensity in Gaussian distribution, as shown in Fig. 1.

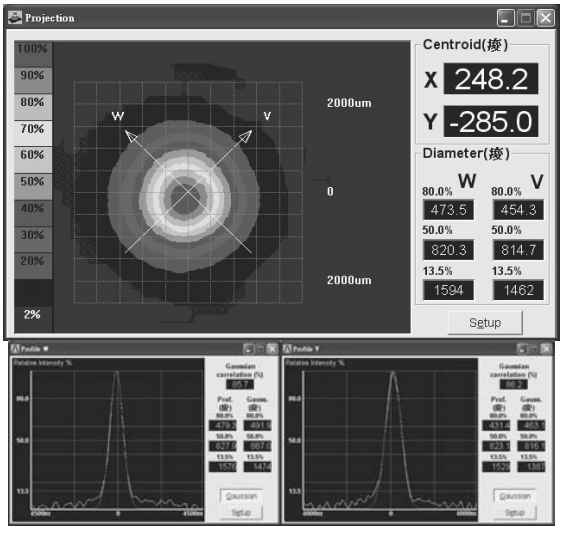

Fig. 1. Laser Projection and Energy Profile

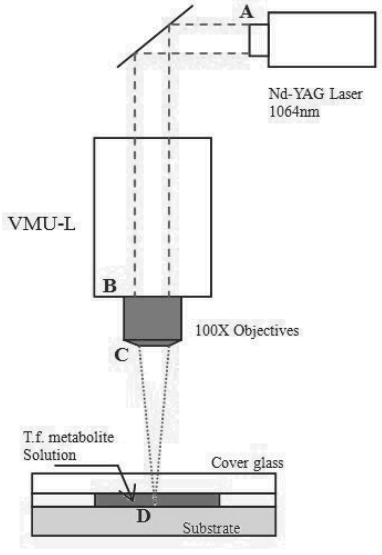

Fig. 2. Schematics of experimental optical setup

Before being focused by 100X objective lens, the laser energy has a distribution detected by 2-dimensional laser projection, and the diameter is 440 μm for 80% energy intensity, 760 μm for 50%, and 1480 μm for 13.5%, respectively. In the current experiment, the optical setup is show in Fig. 2. The laser beam is homogenized and focused through a 100X objective lens then project onto the surface of copper substrate covered with a thin layer of T.f. metabolite solution, as in previous study [7]. The beam diameter on the substrate is defined 7.6 μm.

The associated heat flux of 50% Gaussian distribution energy intensity input is calculated by Eq. (1)-(4), and the adopted parameters are shown in Table 1. In equation (1), the optical intensity $I(r) = |U(r)|^2$ is a function of the axial and radial distances z, and $\rho = (x^2+y^2)^{1/2}$.

$$I(\rho,z) = I_0\left[\frac{W_0}{W(z)}\right]^2 \exp\left[-\frac{2\rho^2}{W^2(z)}\right] \tag{1}$$

The total optical power carried by the beam is the integral of the optical intensity over a transverse plane at a distance z

$$P = \int_0^\infty I(\rho,z)2\pi\rho\, d\rho \tag{2}$$

Since a beam is often specified by its power P, hence Eq. (2) is rewritten

$$I(\rho,z) = \frac{2P}{\pi W^2(z)}\exp\left[-\frac{2\rho^2}{W^2(z)}\right] \tag{3}$$

Table 1.
Parameters of gaussian beam

Item	Construction
ρ	Distance from beam center
ρ_0	Selected radius
U(r)	Complex amplitude
z	Axial distance
P	Total power
W(z)	Beam radius
W_0	Minimum value of beam radius

The ratio of the power carried within a circle of radius ρ_0 on the transverse plane at position z to the total power is:

$$\frac{1}{P}\int_0^{\rho_0} I(\rho,z)2\pi\rho\, d\rho = 1-\exp\left[-\frac{2\rho_0^2}{W^2(z)}\right] \tag{4}$$

Assuming that the one-half peak intensity beam diameter ρ_0 is 760μm, one can find the working input energy is 25.1% of the power source.

The cover glass leads to an absorption of 8.5% energy by PCGrate-S simulation [8]. Accordingly, the optical polar angle in the current experiment is smaller than 5 degree, show in Fig. 3.

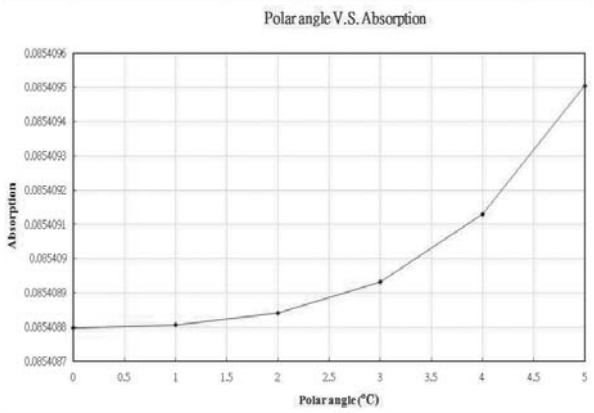

Fig. 3. Relationship between the beam polar angle and absorption (PCGrate-S software)

In the current study, the finite element method is used for analysis of the maskless laser-assisted deposition process by a moving thermal spot on semi-infinity copper substrate. The considered parameters are shown in Table 2 [9]. The element type PLANE77 and the heat flux input in Gaussian distribution are adopted [10]. The deposition reaction occurs with both boiling and forced convection along the heat flux loading side displayed in Fig. 4. The radius of convection effect is iteratively obtained from the temperature distribution of Fig. 5(a) [11,12,13]. The radius of boiling convection is considered 30μm around the laser beam as shown in Fig. 5(b), and the convection effect is set 7000W/m^2*K for laser power of 150mW, 8000W/m^2*K for 180mW, and 9500 W/m2*K for 235mW, respectively, calculated from Nukiyama's boiling curve [10]. The radius of forced convection is considered 300μm as show in Fig. 5(b), and its effect is 3000W/m^2*K for laser power of 150mW, 3500W/m^2*K for 180mW, and 4500W/m^2*K for 235mW, respectively. The values are determined for the thermal flow convection of the medium solution of T.f. as show in Table 3. Due to the increase of laser scanning speed, the forced convection coefficient is estimated to gain 500W/m^2*K at every increase of 5μm/s in scanning speed.

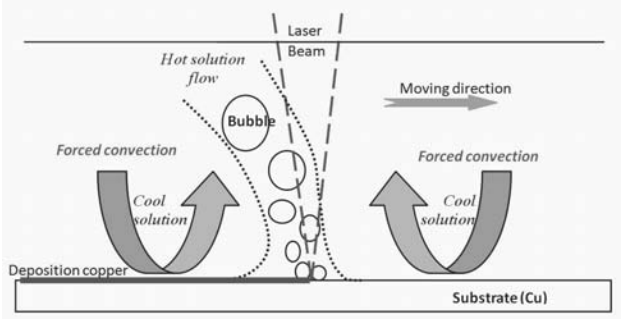

Fig. 4. Boiling and forced convection

The ANSYS Parametric Design Language (APDL) is used for simulation incorporating the specifications of the thermal boundary conditions on 2*2cm^2 work piece at different location and time. The temperature profiles of the same energy input at different scanning speed under theconvection condition are illustrated in Fig. 6(a)(b)(c).

a) Temperature field

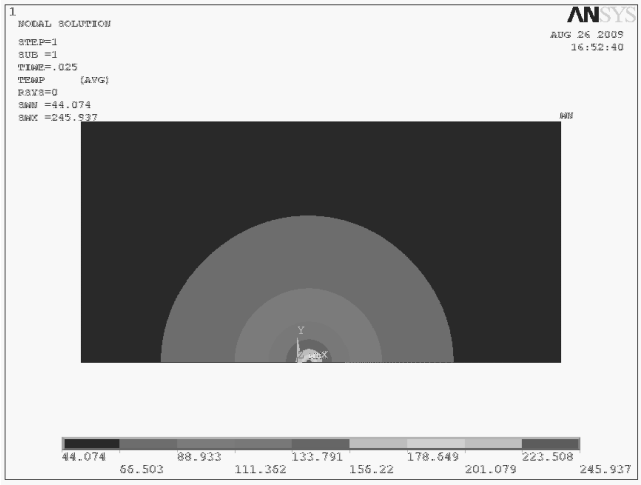

b) Boiling and forced convection near laser source

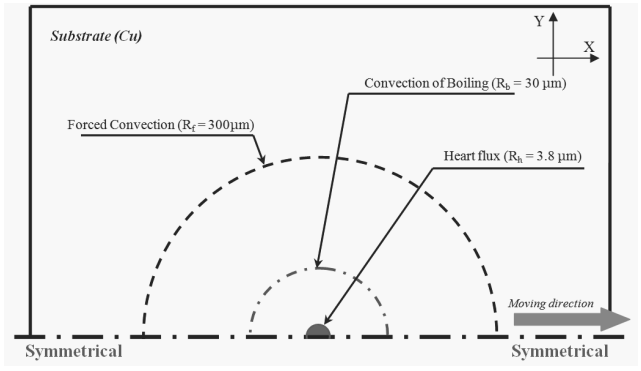

Fig. 5. Numerical analysis schematics (laser power of 150mW, scanning speed of 15μm/s, view size of 300μm*600μm)

Table 2.
Processing parameter in ANSYS

Conductivity (W/m*K)			401
Specific Heat (J/kg*K)			385
Density (Kg/m^3)			8920
Boiling convection coefficient (W/m^2*K)	150mW	180mW	235mW
	7000	8000	9500
Forced convection coefficient (W/m^2*K)			3000~5500
Work piece size			2cm*2cm
Laser power (mW)			150, 180, 235
Velocity (μm/s)			10, 15, 20

One finds the temperature in substrate elevates with increasing laser power and decreasing scanning speed. Under a reasonable assumption that the copper deposition through T.f. metabolite activated by laser irradiation is triggered at a certain

temperature, the above mentioned temperature profile would well indicate the range of deposition to be produced, namely, the width in deposition of lines. Hence the prediction that the deposited line width increases with increasing laser power and decreasing scanning speed can be made by the proposed thermal analysis, and it will be compared with the experimental results.

a)

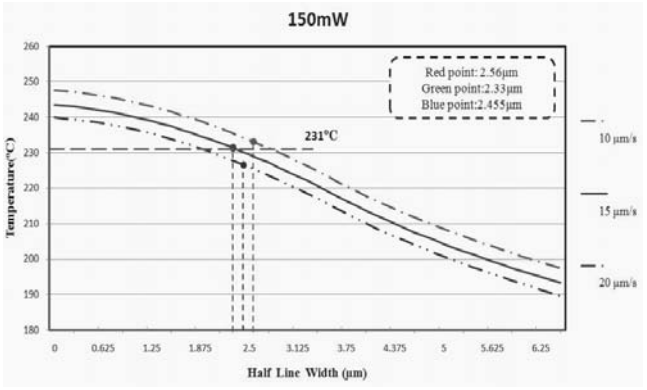

b)

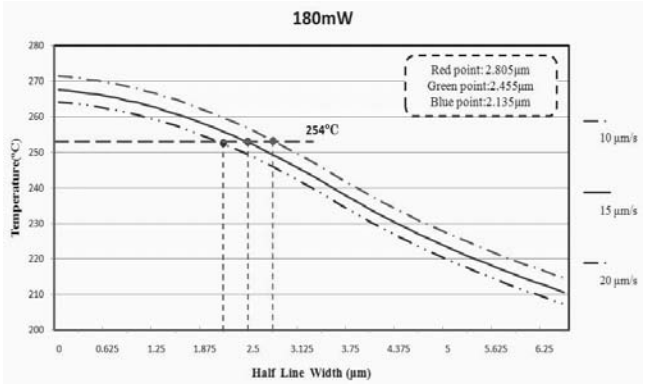

c)

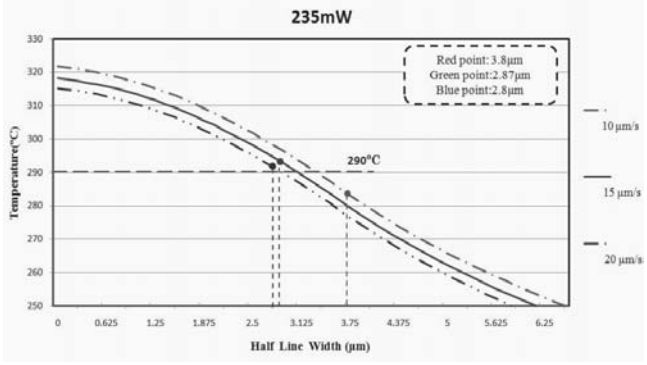

Fig. 6. Temperature profile at different laser power - a) 150 mW, b) 180mW, c) 235 mW

3. Discussion and conclusions

The numerical results of temperature profile are compared with the previous experimental results shown in Table 4. The same trend of the amount of copper deposition, namely positively correlated with laser power and decreased with increasing scanning speed, is demonstrated. Identifying the experimental line width of the deposition in Fig. 6 on the temperature profile, the authors can estimate the temperature at which the deposition through the T.f. metabolite is activated by laser. Fig. 6 shows the activation temperature range is about 260 degree with 30 degree deviation, below that no deposition could be activated. The larger power the laser beam brings in, the higher is the activation temperature. It is presumably attributed to the thermal lead time before the biochemical process is actually started. One can also estimate the limiting speed of laser scanning, higher than that no deposition could occur. The limiting speeds are 30 μm/s, 35 μm/s and 50 μm/s, for 150 mW, 180 mW and 23 5mW, respectively.

Table 3.
Components of solution A and Solution B

Solution A	$(HN_4)_2SO_4$	0.8g
	$MgSO_4 \cdot 7H_2O$	2.0g
	K_2HPO_4	0.4g
	Wolfe's mineral solution	5.0mL
	Distilled water	800mL
Solution B	$FeSO_4 \cdot 7H_2O$	20g
	Distilled water	200mL

Table 4.
Experimental results of laser-assisted deposition

Sample number	Power (mW)	Velocity (μm/s)	Line width (μm)
1	235	10	7.6
2	235	15	5.75
3	235	20	5.6
4	180	10	5.61
5	180	15	4.91
6	180	20	4.27
7	150	10	5.12
8	150	15	4.66
9	150	20	4.91

In Fig. 7, one can see the deposition occurs at the temperature between 230 and 290 degree. At slower scanning speed, the influence of the laser power on the deposited line width is more dominant. The correlation between the deposited line width and the laser power and scanning speed can be illustrated by the current thermal analysis. The produced line width can be predicted along the data fitted line when the laser power and the scanning speed are known. Though the mechanism of the laser-assisted deposition process is not fully revealed yet, the current model provides a means of control of the line deposition of metals. On the fundamental knowledge of how the line width varies with laser power and scanning speed, more investigation of the mini-scale heat convection and the threshold temperature of chemical reaction is expected in the future.

a)

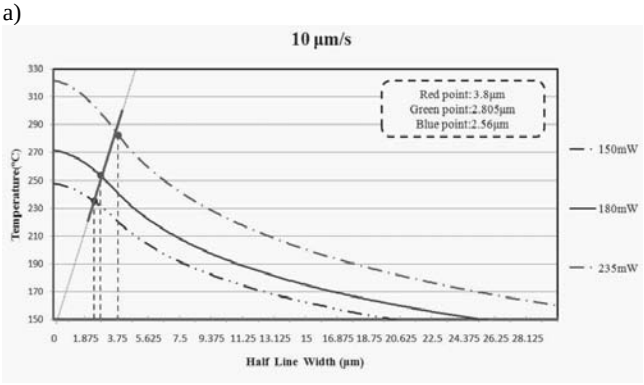

b)

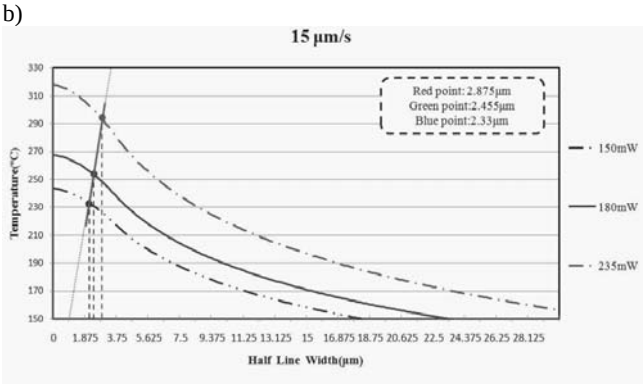

c)

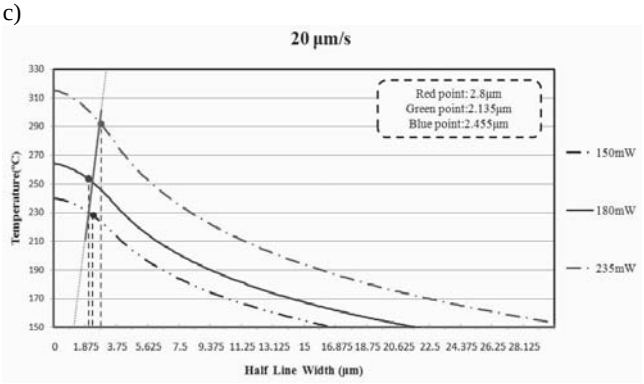

Fig. 7. Temperature profile at different scanning speed- a) 150 mW, b) 180mW, c) 235 mW

References

[1] M.L. Griffith, D.M. Keicher, C.L. Atwood, J.A. Romero, J.E. Smugeresky, L.D. Harwell, D.L. Greene, Proceedings of the Solid Freeform Fabrication Symposium, 1996, Austin, TX, 125.

[2] J. J. Beaman and C. R. Deckard, US patent No. 4938816, 1990.

[3] P.F Jacobs, Rapid Prototyping and Manufacturing, Fundamentals of Stereolithography, Society of Manufacturing Engineers, Dearborn, MI, 1992.

[4] S.D. Allen, Laser chemical vapor deposition: A technique for selective area deposition, Journal of Applied Physics 52/11 (1981) 6501-6505.

[5] H. Hocheng, J.C. Wang, J.H. Chang, W.C. Shen, Laser-guided pattern writing through Thiobacillus ferrooxidans metabolite, Microelectronic Engineering 86 (2009) 565-568.

[6] H. Hocheng, J.H. Chang, H.J. Han, Y.L. Chang, H.Y. Chang, Metal Removal Behavior of Acidithiobacillus Ferrooxidans, AMPT (in press).

[7] Incropera, DeWitt, Bergmann, Lavine, Fundamentals of Heat and Mass Transfer, Sixth edition, John Wiley & Sons(Asia) Pte Ltd, 2007 485-534,619-669.

[8] S.O. Kasap, Optoelectronics and Photonics principles and practices, Pearson prentice Hall, 2001, 87-89.

[9] M. Labudovic, D. Hu, R. Kovacevic, A three dimensional model for direct laser metal powder deposition and rapid prototyping, Journal of materials science 38 (2003) 35- 49.

[10] Incropera, DeWitt, Bergmann, Lavine, Fundamentals of Heat and Mass Transfer, John Wiley & Sons(Asia) Pte Ltd , 2007, 485-534,619-669.

[11] G.E. Thorncroft, J. F. Klausner, The influence of vapor bubble sliding on forced convection boiling heat transfer, Journal of Heat Transfer, February 121/1 (1999) 73-80.

[12] L. Jiang, M. Wong, Y. Zohar, Forced convection boiling in microchannel Heat sink, Journal of Microelectromechanical systems 10/1 (2001) 80-87.

[13] S. Balachandar, D.A. Yuen, D.M. Reuteler, G.S. Lauer, Viscous Dissipation in Three-Dimensional Convection with Temperature-Dependent Viscosity, Science 267/5201 (1995) 1150-1153.